CrossMark

ORIGINAL PAPER

Rockbursting Potential of Kimberlite: A Case Study of Diavik Diamond Mine

Paul Leveille[1] · Mohammadali Sepehri[1] · Derek B. Apel[1]

Abstract The research described in this paper provides information about the rockbursting potential of kimberlite. Kimberlite is a diamond-bearing rock found in deposits around the world including northern Canada. This paper outlines three methods for the prediction of rockbursts based on the properties of a rock. The methods include the: strain energy index, strain energy density, and rock brittleness. Kimberlite samples collected from Diavik, a diamond mine in northern Canada, were tested to define the rock's uniaxial compressive strength, tensile strength, and hysteresis loop. The samples were separated into sub-rock types based on their descriptions from the mine geologists. The results indicate that it is possible to produce rockbursts in kimberlite. It was also observed that the sub-rock types had a range of rockbursting properties. Some types of kimberlite exhibited little to no potential for producing bursts, while other types potentially could produce violent bursts. The diverse nature of kimberlite indicates that the rockbursting properties of the rock should not be generalized and are dependent on the sub-rock type being encountered.

Keywords Rockburst · Kimberlite · Hysteresis · Rock mechanics · Underground mining · Diavik

✉ Derek B. Apel
   dapel@ualberta.ca

1 Department of Civil and Environmental Engineering, School of Mining and Petroleum, University of Alberta, Edmonton, AB T6G 1H9, Canada

1 Introduction

The natural phenomena of rockbursts occur when the stored strain energy in a rockmass is suddenly released causing the expulsion of the material (Blake and Hedley 2003). The effects of a rockburst can vary greatly from minor damage to mine workings and equipment to fatal injuries. Rockbursts occur naturally, but the act of mining can exacerbate the underlying causes, increasing the frequency and magnitude. In general, rockbursts are classified into three main groups: (i) strain burst, (ii) pillar burst, and (iii) fault-slip burst (Fig. 1).

The strain bursts occur at the edge of mine openings when stresses are highly concentrated. This kind of burst often happens in development drifts and shafts, particularly when the drift crosses the contact of a brittle and soft rock. According to Kaiser and Cai (2012), from a loading point of view, two conditions must be met in order for a strain burst to occur: (i) first, in the skin of the excavation, a concentration of the tangential stress (the maximum principal stress) must exist; and (ii) second, the stiffness of the loading system must be soft. If the loading system is softer than the pillar stiffness, the rock fails in a violent manner. The damage from a strain burst can range from the expulsion of rock shards from the wall to the failure of the entire structure.

Pillar bursts occur when the mining-induced stress on a pillar exceeds its strength. The main characteristic of a pillar burst is a violent failure in the pillar core which can even cause the complete collapse of the pillar. Consequently, when the pillar fails, a large amount of strain energy stored in the rock mass will be released violently. Naturally, pillar failures are more susceptible in mining conditions with higher extraction ratios (thus higher stresses), but it is also highly dependent on the geology and natural stress states (Blake and Hedley 2003).
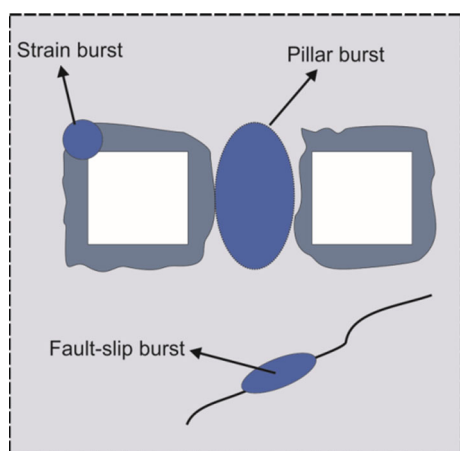
Fig. 1 Schematic representation of rockburst potentials (after Castro et al. 2012)

Fault-slip bursts occur when the frictional resistance created by the normal force is less than the shear stress acting along a geological structure. This type of burst usually occurs in mines with extensively mined out stopes or areas (>1 km^2). Since these large open spaces often expose large geological structures, the magnitude of fault bursts can be very large and can occur at any time (Blake and Hedley 2003). In some cases, the reduction in the normal stress acting on a preexisting fault, as a result of nearby stoping, can cause a fault-slip burst.

Kimberlite is a diamond-bearing igneous rock with a wide range of material properties and compositional characteristics. The rock is mined in northern Canada and is a significant resource for the economy of the local communities and country. Past research into rockbursts developed methods for determining the propensity for bursting from the mechanical properties of a rock. Investigations have been conducted into the bursting properties of many rock types, with considerable focus on coal and granite. However, studies on the rockburst tendencies of kimberlite are nonexistent. Therefore, the goal of this research is to explore this uncharted region to further the scientific understanding of the phenomenon of rockbursting in kimberlite. To meet the objective of this study, an experiment-based research program was conducted on kimberlite samples collected from Diavik diamond mine.

2 Diavik Diamond Mine

2.1 Location

The mine is located on a 20-km^2 island in Lac de Gras, approximately 300 km northeast of Yellowknife, Northwest Territories. Diavik reserves are contained in four diamond-bearing kimberlite pipes named A154 North,

A154 South, A418, and A21, and the host rock is granite. All four pipes were initially located under the waters of Lac de Gras. An aerial view of the mine site can be seen in Fig. 2. The site is extremely remote with only plane access for a majority of the year and ice road access for a few weeks during the harsh winters.

2.2 Underground Mining Methods

The removal of the ore underground utilizes two mining methods: (i) the sub-level retreat (SLR) method and (ii) the blasthole stoping (BHS) method.

Sub-level retreat is a caving-based mining method relying on gravity to feed developed draw points for ore removal. The mining proceeds from the top of the ore body to the bottom with subsequent levels being made to drill, blast, and remove the broken ore. This method relies on gravity to draw the ore to draw points, which is then moved to the surface by equipment.

Blasthole stoping proceeds from bottom to top and involves drilling vertically between two drifts and then blasting off slices of the stope. The opening is then back-filled with a cemented rock to stabilize the opening facilitating the mining of the adjacent stopes. The main difference between BHS and SLR mining methods is that blasthole stoping employs a crown pillar made of ore. The crown pillar is often difficult to completely recover and can result in millions of dollars of potential profit being left in place.

The mining methods employed by an operation can also have an effect on the potential for the production of rockbursts due to the different stresses the different methods can produce. SLR being a caving method would naturally produce greater stresses as it is the intention of the method to create stresses great enough to cause natural failure of the ore, whereas blasthole stoping helps in alleviating the increase in the stresses by backfilling the stopes with waste material. However, blasthole stoping being a bottom-up method has a greater amount of material overlying the mining levels compared to SLR mining levels which operate much closer to the surface.

2.3 Geology

There are two main rock types faced in the mining of the diamond pipes at Diavik: granite and kimberlite. The diamond pipes are made of the kimberlite surrounded by the considerably older granite, known as the Canadian Shield.

The kimberlite samples collected were grouped into seven sub-rock types determined by the geologists working at the mine. The sub-rock types were differentiated based on formation, grain size, matrix composition, and strength. Kimberlite is known for its high variability and

Fig. 2 Aerial view of Diavik diamond mine (courtesy of Diavik diamond mine, (Rio Tinto 2015))

Table 1 Kimberlite sub-rock type codes and geological descriptions

Kimberlite pipe	Rock code	Geological description
A154 South	PK	Pyroclastic kimberlite
	PKX	Olivine and macrocryst-rich pyroclastic kimberlite
A154 North	MK	Magnetic lapilli-rich macrocrystic volcaniclastic kimberlite
	BMVK	Black macrocrystic volcaniclastic kimberlite
	MRK	Mud-rich volcaniclastic kimberlite
	HK	Coherent kimberlite

unpredictable nature, which is why each kimberlite pipe has many sub-rock types differentiated. The list and description of the rock types received from Diavik can be seen in Table 1.

3 Rockburst Prediction Methods

There are four popular indicators that have been developed to measure the bursting behavior of a rock: (i) strain energy index, (ii) strain energy density, (iii) rock brittleness, and (iv) tangential stress. Only the first three indicators were utilized in this research on kimberlite and are described in detail below.

4 Strain Energy Index Method

The strain energy index (W_{ET}) is a dimensionless ratio of the stored elastic energy to dissipated elastic energy from a hysteresis loop of a rock specimen as shown in Fig. 3. The formula for the W_{ET} is given by Eq. (1), where the symbols
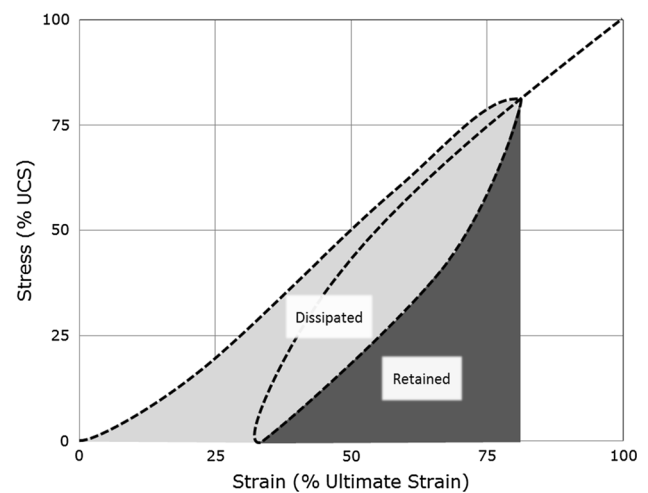

Fig. 3 Hysteresis loop indicating the dissipated and retained energy regions (after Wattimena et al. 2012)

φ_{sp} and φ_{st} represent the values for the strain energy retained and strain energy dissipated, respectively.

$$W_{ET} = \varphi_{sp} / \varphi_{st} \qquad (1)$$

Table 2 Strain energy index classifications

Strain energy index	Mode of fragmentation
$W_{ET} < 2$	Brittle fragmentation
$2 \leq W_{ET} < 5$	Transitional failure
$5 \leq W_{ET}$	Violent failure

A hysteresis loop is produced by loading a sample to 80–90% of the uniaxial compressive strength (UCS) and then completely releasing the stress at the same rate. According to Kidybinski (1981), the strain energy index corresponds to three possible classifications for fragmentation as described in Table 2. The strain energy index is based on the assumption that a rockburst releases mechanical energy proportional to the elastic strain energy stored in a unit volume of rock.

4.1 Strain Energy Density Method

The strain energy index method works well for materials that exhibit plastic strain behavior. However, other rocks (for example granite) will often only have elastic strain during a hysteresis loop which is consequently difficult to measure with the strain energy index method. The strain energy density method (SED, kJ/m³) utilizes the unloading tangential modulus (E_s, GPa) from the hysteresis loop and the uniaxial compressive strength (σ_c, MPa). The unloading tangential modulus can be seen in Fig. 4 as the tangent to the initial portion of the unloading curve, and the calculation of the SED is given by Eq. (2). The strain energy density method is based on the assumption that the test specimen is linearly elastic.

$$\text{SED} = \sigma_c^2 / (2E_s) \tag{2}$$

Table 3 provides a qualitative hazard potential for a rockburst to occur based on the SED for a particular rock. The classifications are based on studies of hard rock samples.

4.2 Rock Brittleness Method

The rock brittleness method (RB) is the most simple to calculate; it is the ratio of the uniaxial compressive strength (σ_c) to the tensile strength (σ_t) as shown in Eq. (3). From experimental results and site investigations, it was found that the strength of a rockburst could be defined based on the rock brittleness value and corresponding classifications in Table 4 (Wang and Park 2001). The idea behind this method is that the greater the uniaxial compressive strength is, compared to the tensile strength, the weaker the burst is that can be produced.

$$B = \sigma_c / \sigma_t \tag{3}$$
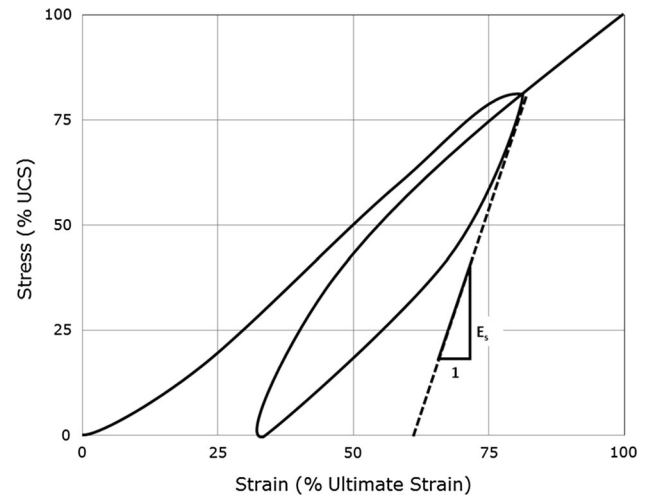
Fig. 4 Hysteresis loop indicating the unloading tangential modulus (after Wang and Park 2001)

Table 3 Strain energy density and hazard potential classifications (after Wang and Park 2001)

Strain energy density (kJ/m³)	Hazard potential
SED ≤ 50	Very low
50 < SED ≤ 100	Low
100 < SED ≤ 150	Moderate
150 < SED ≤ 200	High
200 < SED	Very high

Table 4 Rock brittleness classifications

Brittleness value	Burst strength
$B < 14.5$	Violent
$14.5 \leq B < 26.7$	Strong
$26.7 \leq B < 40$	Weak
$40 \leq B$	None

5 Experimental Procedures

In order to determine the rockbursting properties of kimberlite samples, it is required to conduct three distinct tests. The experiments included: uniaxial compressive strength (UCS) tests, Brazilian tensile strength (BTS) tests, and cyclic loading tests.

The uniaxial compressive strength tests were conducted in compliance with ASTM D7012-13 (2013)—compressive strength and elastic moduli of intact rock. These experiments were conducted using two different machines depending on the size of the cores. The larger cores (63.5-mm-diameter cores) were tested using the 1000-ton servo-hydraulic controlled INSTRON loading frame, and the
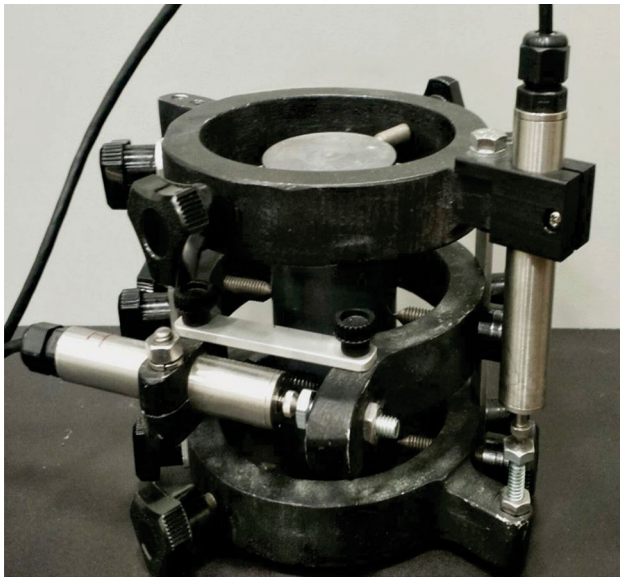
Fig. 5 Compressometer with LVDT arrangement for vertical and horizontal deformation measurements

Fig. 6 Brazilian tensile strength test equipment

Fig. 7 Loading pattern for the cyclic loading tests (after Leveille 2016)

vertical and horizontal deformations were measured using a compressometer with linear variable differential transducers (LVDT) shown in Fig. 5. The other tests were conducted using a MTS loading frame, and the deformation measurements were taken by strain gauges. The results from these experiments were used to determine the UCS, Young's modulus, and Poisson's ratio of each rock type.

The tensile strength of the samples was determined using the Brazilian tensile strength test (also referred to as the splitting tensile strength test). The procedure for the experiment as well as the preparation of the samples was obtained from ASTM D3967-08 (2008), the Standard Test Method for Splitting Tensile Strength of Intact Rock Core Specimens. The apparatus to hold and position the specimen under the loading frame is shown in Fig. 6. There are two steel loading jaws designed to contact the disk-shaped rock specimen at diametrically opposed surfaces.

The method for conducting the cyclic loading tests was based on the description given by Kidybinski, by loading the sample to 80–90% of the sample's UCS, then unloading completely and then reloading to failure (Kidybinski 1981). Being able to predict the UCS of a rock with any kind of accuracy can be quite difficult without a large number of samples. Due to the limited number of samples, it was decided to cyclically load the sample in 25% increments of the average UCS strength to attempt to ensure a viable cycle would be produced. The loading rate was based on the guidelines given by ASTM D7012-13 (2013) since the cyclic loading test was also a compressive test. The loading and unloading of the sample were done at the same rate which was 0.5 MPa/s, and since the strength of the sample
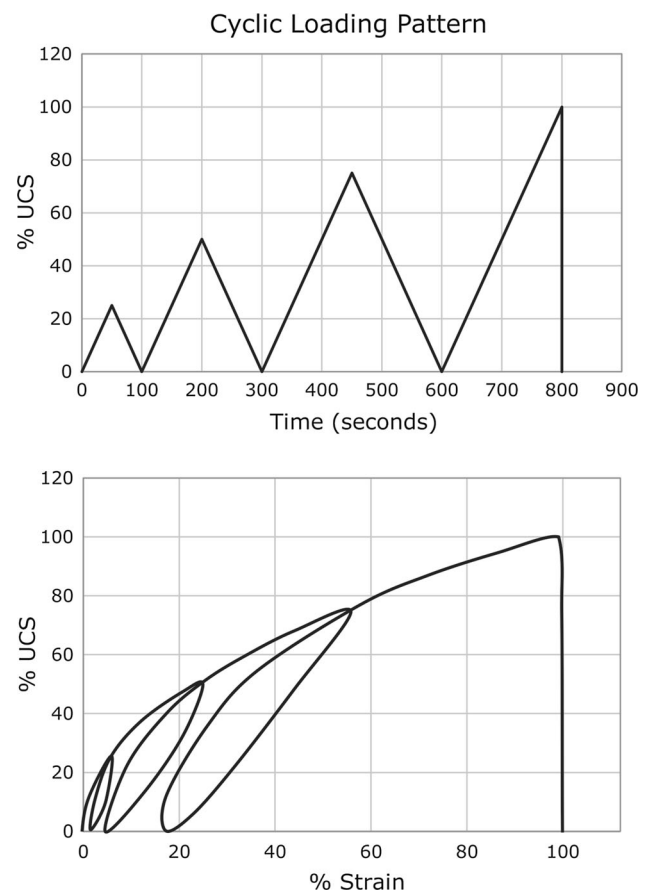
could not be estimated with great accuracy, the loading was done in 25% incremental increases until sample failure; an example of the loading pattern is shown in Fig. 7. The loading pattern was done in such a way to obtain the load/ unload cycle between 70 and 90% UCS of the sample.

Table 5 Type and quantity of samples prepared

| Rock type	UCS	BTS	Cyclic loading
PK	3	3	3
PKX	3	7	3
MK	3	6	3
BMVK	3	7	3
MRK	3	6	1
HK	3	5	0

5.1 Sample Preparation

The rock types and quantity of samples prepared are shown in Table 5. The samples were prepared by coring rock samples collected from the active mining faces. A minimum of three samples for each experiment was prepared from the provided kimberlite. In the case of rock types MRK and HK, the samples would not produce enough acceptable cores for testing.

6 Results

The results from the experiments and calculations are presented in Table 6. Any space in the table with a dash in place of data was because of insufficient samples to conduct the tests on the particular sub-rock type. Furthermore, the calculations of the rockbursting indicators were done using the results from the cyclic loading tests and not from the results of the UCS and BTS experiments. The UCS and BTS averages were calculated using only the results from those tests and do not include the cyclic loading test data.

The hysteresis loop for each sample was found by performing a cyclic loading test. The samples were loaded and then unloaded in 25% increments based on the rock type's UCS until the sample failed. To ensure the sample experienced consistent load cycling, the load was applied and released at the same rate. The information collected from each test looks similar to Fig. 8; the title MK-UCS4 indicates the rock type and the sample ID, which in this case is
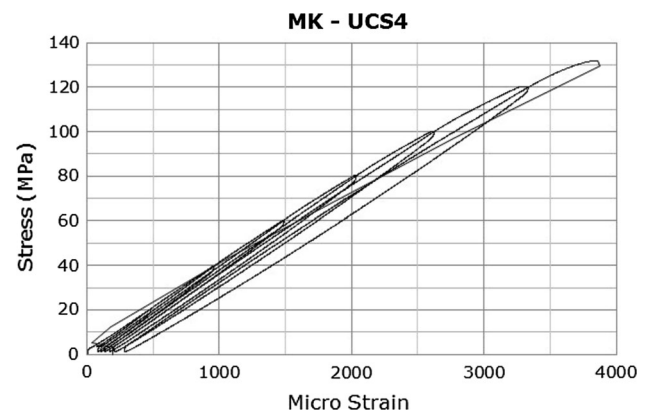
Fig. 8 Cyclic loading experiment for MK—UCS4

UCS4. The figure shows the incremental loading pattern described and the residual strain in the sample when it is unloaded each time. An interesting and an encouraging sign of the measurements quality can be seen when load was reapplied; each time the load was reapplied, the stress–strain curve crossed through the peak of the previous loading cycle, indicating that the strain measurement device was still properly attached to the sample.

From the information obtained from the graphs similar to Fig. 8, the analyzed data were limited to the loading cycle which satisfied the 70–90% of the ultimate strength of the sample. The data were reduced by removing all the unloading cycles and appending all the loading cycles together to produce the hysteresis loops such as the sample shown in Fig. 9. The slope of the unloading curve is also shown in the graph as a red line and represents the unloading modulus, which is used in the determination of the rockbursting properties.

The classification of the rockbursting properties for each rockburst indicator is given in Table 7. Any data replaced with a dash are the result of insufficient samples to complete the proper tests for the rock type. The overall rock type is the overall rating for the kimberlite rock type tested. The overall rating of the kimberlite for the strain energy index, strain energy density, and rock brittleness methods is transitional, low/moderate, and strong, respectively.

Table 6 Summary of quantitative results

Rock type	UCS (MPa)	BTS (MPa)	E (GPa)	E_s (GPa)	W_{ET}	SED	RB
PK	63.8	3.0	19.9	31.3	2.4	96	22.4
PKX	69.4	3.7	18.5	35.3	2.4	87	18.9
MK	80.7	4.4	26.2	44.3	3.5	149	22.3
BMVK	58.3	3.0	17.7	46.2	1.9	29	15.2
MRK	45.6	3.5	10.0	41.8	3.4	181	11.7
HK	70.4	9.7	39.6	–	–	–	7.3

Fig. 9 Hysteresis loop from cyclic loading test on MK—UCS4
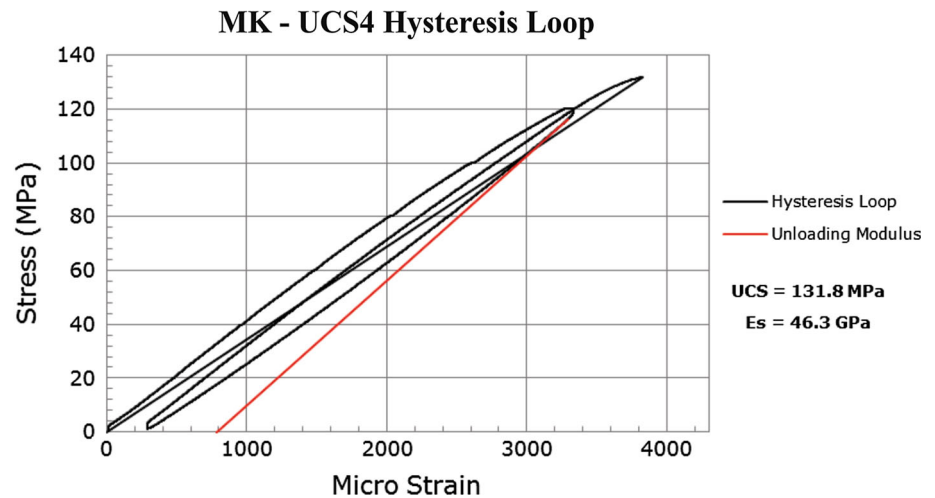
Table 7 Rockbursting classifications for sub-rock types

Rock type	WET	SED	RB
PK	Transitional	Low	Strong
PKX	Transitional	Low	Strong
MK	Transitional	Moderate/high	Strong
BMVK	Brittle	Very low	Strong
MRK	Transitional	High	Violent
HK	–	–	Violent
Overall	Transitional	Low/moderate	Strong

Table 8 Combined rating system conversion

WET	SED	RB
Brittle = 0	Very low = 0	None = 0
Transitional = 1	Low = 1	Weak = 1
Violent = 2	Moderate = 2	Strong = 2
	High = 3	Violent = 3
	Very high = 4	

7 Discussion

The results from the rockburst investigation varied for the different sub-rock types of kimberlite. PK and PKX both were found in A154 South pipe, produced the same rockburst ratings, and should thus produce similar rockbursts under the same stress conditions. The similarity of the rockburst characteristics between PK and PKX means that the two rock types are equally likely to burst, and the same consideration should be taken when placing rockburst mitigating techniques in this pipe.

The sub-rock types from A154 North (MK, BMVK, MRK, and HK) produced more varied results than those from A154 South pipe. This is probably due to the mudrock intrusions in these samples (letter M indicates mudrock intrusion). Therefore, the rockbursts that could be generated in A154 North pipe will vary depending on the sub-rock type in which they occur. During mining of an underground level in which several of these rock types are encountered, the sub-rock type more prone to bursting should be of greater concern when designing the mine, planning the mining sequence, and implementing rockburst mitigation techniques.

The qualitative results are beneficial for understanding the nature of the rockbursting properties of each sub-rock type, but comparing the rockbursting propensity of the sub-rock types is challenging. A quantitative comparison method would make this considerably easier. Table 8 illustrates how the bursting indicators can be converted into numeric ratings.

The values from the conversion for each sub-rock type and rockburst indicator are then used in a calculation to create an overall combined rockburst rating for each of the types of kimberlite. The combined rating is calculated by dividing the converted values of the three rating systems by their respective maximum potential converted value. An equally weighted average of the three indicators for each sub-rock type is found, and the result is multiplied by 100, to create a rating out of 100. The calculation of the combined rating value for PK can be seen in Appendix as an example. The converted rockburst indicator values and corresponding combined ratings can be seen in Table 9. The combined rating for HK is not representative since this value is based on only the rock brittleness value and does not include the other rockburst indicators.

Comparing the rockbursting propensity of the sub-rock types is much clearer now with the combined ratings. The combined ratings can then be used for producing a color-coded rockburst map of the orebody based on the sub-rock type. The information gained from the combined rating

Table 9 Combined ratings for sub-rock types

Rock type	W_{ET}	SED	RB	Combined rating
PK	1	1	2	47
PKX	1	1	2	47
MK	1	2	2	56
BMVK	0	0	3	33
MRK	1	3	3	75
HK	–	–	3	100
Overall	1	1.4	2.5	56
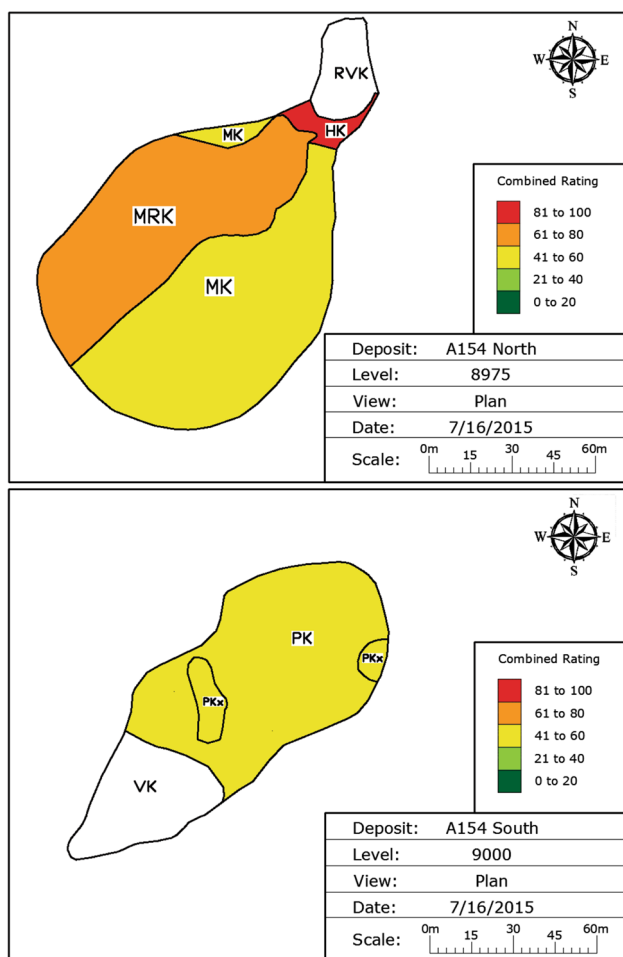
Fig. 10 Combined ratings cross sections for north and south pipe rock types (After Leveille 2016)

system would be useful when choosing a mining method, designing underground workings, production sequencing, and deciding on the appropriate rockburst mitigation methods to utilize. Rockburst maps can be created to highlight the different ratings of the sub-rock types and spatial relations. Two cross section examples of such maps can be seen in Fig. 10. The maps show the greater variety in the rockburst rating found in the North pipe compared to

the South pipe. The areas of the pipe that are not filled in represent areas with unknown rockburst properties. These maps provide a valuable tool to mitigate rockbursts from occurring during the planning process. While planning, a planner can determine an optimal approach and sequencing for the level based on the rockburst ratings.

8 Conclusions

Experiments were conducted on sub-types of kimberlite collected from a Canadian diamond mine to gain an understanding of the rockbursting properties of kimberlite. The experiments included: uniaxial compression tests, Brazilian tensile strength tests, and cyclic loading tests; the results from these experiments were used to analyze the rockbursting properties for the kimberlite in general as well as the sub-rock types of kimberlite. The test results show that kimberlite in general has the potential to produce rockbursts based on the rating systems used in this research. Diversity in the rockbursting properties was also found among the distinct kimberlite sub-rock types. Some of the sub-rock types had considerably high combined ratings, indicating that the potential for kimberlite to generate violent rockbursts exists. The wide range of results for the sub-rock types of kimberlite indicates that kimberlite should not be treated as a single rock type when considering the potential for rockbursts in an orebody, but rather the rockbursting potential of all the sub-rock types should be assessed.

Appendix

Combined rating = Average $[(1/2), (1/4), (2/3)] \times 100$

Combined rating = Average $[0.5, 0.25, 0.667] \times 100$

Combined rating = 0.47×100

Combined rating = 47

References

ASTM D3967-08 (2008) Standard test method for splitting tensile strength of intact rock core specimens

ASTM D7012-13 (2013) Standard test methods for compressive strength and elastic moduli of intact rock core specimens under varying states of stress and temperatures

Blake W, Hedley DG (2003) Rockbursts: case studies from North American hard-rock mines. Society for Mining Metallurgy, and Exploration, Englewood

Castro LM, Bewick RP, Carter TG (2012) An overview of numerical modelling applied to deep mining. In: Azevedo R (ed) Innovative numerical modelling in geomechanics. CRC Press, London, pp 393–414

Kaiser PK, Cai M (2012) Design of rock support system under rockburst condition. Journal of Rock Mechanics and Geotechnical Engineering 4(3):215–227

Kidybinski A (1981) Bursting liability indices of coal. International Journal of Rock Mechanics Mineral Sciences Geomechanics 18:295–304

Leveille P (2016) Rockbursting properties of Kimberlite—Diavik diamond mine case study. Master of Science Thesis, University of Alberta

Rio Tinto (2015) Photo library—Rio Tinto, 2015. [Online]. Available: http://www.riotinto.com/media/photo-library-263.aspx?y=1492

Wang J-A, Park H (2001) Comprehensive prediction of rockburst based on analysis of strain energy in rocks. Elsevier, Seoul

Wattimena RK, Sirait B, Widodo NP, Matsui K (2012) Evaluation of rockburst potential in a cut-and-fill mine using energy balance. International Journal of the Japanese Committee for Rock Mechanics 1:19–23